


A novel assay for measuring recombinant human lysophosphatidylcholine acyltransferase 3 activity

Xinming Du¹, Jiachun Hu² , Qing Zhang³, Qi Liu², Xinxin Xiang², Jibin Dong², Bin Lou², Shuhua He², Xiang Gu², Yu Cao⁴, Yingxia Li¹ and Tingbo Ding²

1 Department of Medicinal Chemistry, School of Pharmacy, Fudan University, Shanghai, China

2 Department of Pharmacology and Biochemistry, School of Pharmacy, Fudan University, Shanghai, China

3 Shanghai Science Research Center, CAS Center for Excellence in Molecular Cell Science, Shanghai Institute of Biochemistry and Cell Biology, Chinese Academy of Sciences, University of Chinese Academy of Sciences, Shanghai, China

4 Institute of Precision Medicine, The Ninth People's Hospital, Shanghai Jiao Tong University School of Medicine, China

Keywords

enzyme kinetics; inhibitor screening; LPCAT3; lysophosphatidylcholine acyltransferase 3; sequential mechanism

Correspondence

T. Ding, Department of Pharmacology & Biochemistry, school of pharmacy, Fudan University, Shanghai, China

E-mail: tbding@shmu.edu.cn

Y. Li, Department of Medicinal Chemistry, School of Pharmacy, Fudan University, Shanghai, China

E-mail: liyx417@fudan.edu.cn

Y. Cao, Institute of Precision Medicine, the Ninth People's Hospital, Shanghai Jiao Tong University School of Medicine, Shanghai, China

E-mail: yu.cao@shsmu.edu.cn

Lysophosphatidylcholine acyltransferase 3 (LPCAT3) is an important enzyme in phospholipid remodeling, a process that influences the biophysical properties of cell membranes and thus cell function. Multiple lines of evidence suggest that LPCAT3 is involved in several diseases, including atherosclerosis, non-alcoholic steatohepatitis, and carcinoma. Thus, LPCAT3 may have potential as a therapeutic target for these diseases. In the present study, we devised an assay based on reversed-phase HPLC to measure LPCAT3 activity, which may facilitate the identification of LPCAT3 inhibitors and activators. We found that optimal pH and temperature of recombinant human LPCAT3 are 6.0 and 30 °C, respectively. The enzyme K_m values for substrates NBD-labelled lysophosphatidylcholine and arachidonoyl CoA were 266.84 ± 3.65 and $11.03 \pm 0.51 \mu\text{mol}\cdot\text{L}^{-1}$, respectively, and the V_{max} was $39.76 \pm 1.86 \text{ pmol}\cdot\text{min}^{-1}\cdot\text{U}^{-1}$. Moreover, we used our new method to determine the IC_{50} of a known LPCAT inhibitor, TSI-10. In conclusion, this novel assay can be used to measure the effects of compounds on LPCAT3 activity.

Xinming Du and Jiachun Hu contributed equally to this work.

(Received 4 June 2019, revised 2 July 2019, accepted 2 August 2019)

doi:10.1002/2211-5463.12712

Phospholipids are a major constituent in the cell membrane. The fatty acyl composition in phospholipids has an impact on the biophysical properties of the cell membrane and, consequently, the cell response to ambient stimuli. The majority of *de novo* synthesized phospholipids, which are composed of a saturated fatty acyl

group in the *sn*-2 position of the glycerol backbone, are matured by the Lands cycle, a remodeling pathway, in which the saturated fatty acyl group in the *sn*-2 position is replaced by polyunsaturated acyl group upon the action of phospholipase A2 and lysophosphatidylcholine acyltransferase, respectively [1]. Among the four

Abbreviations

Ara-CoA, arachidonoyl coenzyme A; Bi-Bi, bisubstrate-biproduct, DDM, *N*-dodecyl- β -D-maltopyranoside; NBD-lyso-PC, NBD-labelled lysophosphatidylcholine; NBD-PC, NBD-labelled phosphatidylcholine; rhLPCAT3, recombinant human lysophosphatidylcholine acyltransferase 3; SEC, size exclusion chromatography.

isoforms identified so far, lysophosphatidylcholine acyltransferase 3 (LPCAT3) is of intensive interest because of its unique status in lipid metabolism. Expression of LPCAT3 is regulated by intracellular lipid homeostatic regulators such as PPAR α , PPAR δ and LXR [2–5]. LPCAT3 is the major isoform in liver, small intestine, adipose tissue and macrophages [6–9]. LPCAT3 activities determine the polyunsaturated fatty acyl composition in these tissues and cells. *Ex vivo* experiments have suggested that LPCAT3 activity is involved in small intestine tumorigenesis, macrophage polarization, hepatocyte apoptosis, adipocyte differentiation and adipogenesis [9–12]. *In vivo* experiments in mice indicate that LPCAT3 deficiency in small intestine has a dominant effect over its deficiency in the liver with respect to reducing plasma triglyceride and cholesterol levels because of the affected lipid absorption by small intestine [13]. Mass spectrometry analysis in lesions and transplantation of LPCAT3 knockout hematopoietic cells into LDLR knockout mice suggest that LPCAT3 activity is associated with atherosclerosis [8,14,15]. Followed by decreased LPCAT3, hepatocyte death mediated by the lipotoxicity effect of accumulated lyso-PC may be the cause of non-alcoholic steatohepatitis in mice fed a high-fat diet with sucrose [11]. Accumulating evidence suggests that pharmacological manipulation of LPCAT3 activity might provide novel therapeutic methods with respect to the pathological state of atherosclerosis, non-alcoholic steatohepatitis, carcinoma, and immuno- and inflammatory disorders, etc. [16].

To screen compounds that regulate LPCAT3 activity, we purified a recombinant human LPCAT3 protein expressed in insect cells and then developed a reversed-phase HPLC with a fluorescence detector method to quantify the catalytic product of this enzyme and determine its activity. By this method, we obtained the K_m of the substrate NBD-labelled lysophosphatidylcholine (NBD-lyso-PC) and arachidonoyl coenzyme A (Ara-CoA) under conditions of optimal pH and temperature. A sequential bisubstrate–biproduct (Bi–Bi) kinetic mechanism of this enzyme could also be proposed via Lineweaver–Burk plots. Furthermore, we determined the IC_{50} of the LPCAT3 inhibitor in catalytic reactions with refined concentrations of enzyme and substrates, which could be applied to screen LPCAT3 regulators in the laboratory.

Materials and methods

Materials

NBD-lyso-PC/NBD-labelled phosphatidylcholine (NBD-PC) was purchased from Avanti Polar Lipids Inc.

(Alabaster, AL, USA). Ara-CoA was purchased from Sigma-Aldrich (St Louis, MO, USA) NBD-lyso-PC/NBD-PC/Ara-CoA were dissolved in methanol and stored at $-20\text{ }^{\circ}\text{C}$. BSA was obtained from Solarbio (Beijing, China). *N*-dodecyl- β -D-maltopyranoside (DDM) was purchased from Anatrace (Maumee, OH, USA). The bicinchoninic acid protein assay kit was purchased from Beijing ComWin Biotech Co. Ltd (Beijing, China). High-performance Silica gel TLC plates (20 cm \times 20 cm, 0.2-mm gel thickness) were obtained from Yantai Jiangyou silicone development company (Shandong, China). TSI compounds were reported by Megumi Tarui as selective LPCAT2 inhibitors [17] and were synthesized by Xinming Du from the Department of Medicinal Chemistry of Fudan University (Shanghai, China). Chromatographic grade acetonitrile and methanol were purchased from Cinc High Purity Solvents Co. Ltd (Shanghai, China). Trifluoroacetic acid, chloroform and other regular reagents were purchased from Sino-pharm Chemical Reagent Co. Ltd (Shanghai, China).

Methods

Preparation and identification of the recombinant hLPCAT3

The coding cassette of human LPCAT3 gene (BC065194.1) was achieved by RT-PCR with template RNA from cells of a human source before being cloned into pFAST-Bac-Rn plasmid with a Twin-strep-tag (WSHPQFEKGGG-SGGGSGG-SAWSHQPFEK) on the C terminus and a HRV 3C protease cleave site (LEVLFQ¹GP) between hLPCAT3 and the tag. The recombinant plasmid was named pFAST-HC-S-hLPCAT3 and confirmed by sequencing. Bacmid and baculoviral of LPCAT3 were generated, and P3 viruses were used to infect Sf9 cells. Infected cells were harvested within 48 h and the membranes proteins were isolated: cells were suspended in 100 mL of low salt buffer (10 mM NaCl, 10 mM Hepes, pH 7.5, 1 mM phenylmethanesulfonyl fluoride) and then the pellet was collected after centrifugation at 45 000 *g* and 4 $^{\circ}\text{C}$ for 25 min. The pellet was resuspended in high salt buffer (1 M NaCl, 25 mM Hepes, pH 7.5, 1 mM phenylmethanesulfonyl fluoride, 5 mM MgCl₂, 1 \times Cocktail DNase) and homogenated until no visible particles could be seen. The mixture was centrifuged at 45 000 *g* and 4 $^{\circ}\text{C}$ for 25 min. Then, the pellet was further suspended in 50 mL lysis of buffer (150 mM NaCl, 20 mM Hepes, pH 7.5, 10% glycerol, 1 mM phenylmethanesulfonyl fluoride, 5 mM MgCl₂, 1 \times Cocktail DNase) and homogenated until no visible particles could be seen. After DDM was added to a final concentration of 1.5% w/v, the mixture was gently shaken for 2 h to help the membrane protein dissolve. The membrane protein was prepared in the supernatant after centrifugation at 45 000 *g* and 4 $^{\circ}\text{C}$ for 45 min. The recombinant hLPCAT3 protein was further purified from the membrane proteins using the

Strep-tag[®] system (IBA GmbH, Göttingen, Germany): after the Strep-Tactin[®]XT Superflow[®] (IBA GmbH) resin was balanced successively with 10 mL of lysis buffer (150 mM NaCl, 20 mM Hepes, pH 7.5, 10% glycerol) and 10 mL of 2 mM DDM lysis buffer (150 mM NaCl, 20 mM Hepes, pH 7.5, 10% glycerol, 2 mM DDM), the supernatant containing membrane proteins was loaded onto the resin at a flow of 0.5–1 mL·min⁻¹. The resin was washed twice with 10 mL of 2 mM DDM lysis buffer and then eluted using 3–4 mL of elution buffer (150 mM NaCl, 20 mM Hepes, pH 7.5, 10% glycerol, 2 mM DDM, 5 mM desthiobiotin). The eluate was further purified by size exclusion chromatography (SEC) (GE AKATA Pure[®] system with a column of Superdex 200 Increase 10/300 GL; GE Healthcare Life Sciences, Chichago, IL, USA). The mobile phase (150 mM NaCl, 20 mM Hepes, pH 7.5, 1 mM DDM) for SEC was set as a flow of 0.4 mL·min⁻¹. Fractions of SEC that contain LPCAT activities were finally combined as the purified hLPCAT3 enzyme. The protein concentration was measured by the bicinchoninic acid method and the purity of this recombinant hLPCAT3 protein was identified by SDS/PAGE combined with Coomassie Brilliant Blue G250 staining. The activity of this purified recombinant hLPCAT3 was determined by the formation rate of the product NBD-PC.

Isolation of liver microsomal proteins as the source of LPCAT3

Mice (10 weeks old) on a C57BL/6 background were purchased from Shanghai Model Organisms Center, Inc (Shanghai, China). Experimental mice were housed under a 12:12 h light/dark cycle in a temperature- and humidity-controlled room. Mice were fed a chow diet. Experiments involving mice were conducted with the approval of Fudan University Institutional Animal Care and Use Committee. The procedures followed were in accordance with institutional guidelines.

Mice were sacrificed using cervical dislocation and liver tissue were dissected, weighed and then homogenized in 100 mM Tris-Cl pH 7.4 containing protease inhibitor cocktail (Sigma-Aldrich). After centrifugation for 10 min at 9000 *g*, the supernatants were collected and centrifuged at 100 000 *g* for 1 h at 4 °C. The resultant pellets (microsomal proteins) were resuspended in 100 mM Tris-HCl (pH 7.4) containing protease inhibitor cocktail (Sigma-Aldrich) and stored at -80 °C. The concentration of the liver microsomal proteins was determined by the bicinchoninic acid method.

General enzymatic reaction of rhLPCAT3

A general enzymatic reaction of 100 µL was incubated at 30 °C for 10 min, which contained 1 mg·mL⁻¹ BSA, 75 mM Tris-Cl (pH 6.0), 1 mM DDM, 100 µmol·L⁻¹ NBD-lyso-PC, 100 µmol·L⁻¹ Ara-CoA and one-unit of purified

recombinant human LPCAT3 (rhLPCAT3) enzyme. One-unit of rhLPCAT3 activity was defined in this article as the amount of enzyme required to generate 25 pmol NBD-PC·min⁻¹ under the above conditions.

Analysis of NBD-PC by TLC or reversed-phase HPLC

For analysis of NBD-PC by reversed-phase HPLC, the reaction was terminated using 100 µL of acetonitrile. After vortexing for 15 s, the reaction mixture was centrifuged at 9000 *g* for 10 min and 20 µL of supernatant was used for the HPLC analysis. HPLC was performed with an HC-C18 column (250 mm × 4.6 mm, 5 µm) (Agilent Technologies Inc., Santa Clara, CA, USA) and an isocratic elution with methanol/water/trifluoroacetic acid (94:6:0.04, v/v). The flow rate of the mobile phase was set as 1.0 mL·min⁻¹. Detection was accomplished with a fluorescence spectrophotometer (excitation wavelength of 475 nm, emission wavelength of 525 nm). The photomultiplier tube gain was 12. All of the product NBD-PC in the present study was measured by reversed-phase HPLC.

For analysis of NBD-PC by TLC, the reaction was terminated by adding 300 µL of chloroform/methanol (1:1, v/v) and vortexing. The lower organic phase was collected and dried under nitrogen gas after 15 s of vortexing and 10 min of centrifugation at 9000 *g*. Residual lipids were redissolved in 40 µL of chloroform/methanol (2:1, v/v) and applied to a TLC plate, which was then developed using chloroform/methanol/H₂O (65:25:4, v/v/v). The fluorescence signal was detected under UV.

Calibration curve of NBD-PC

The calibration curve of the external standard method was used for the quantification of NBD-PC. The calibration curve was constructed by plotting the peak area of product (NBD-PC) (*y*) versus NBD-PC concentration (*x*). The regression parameters of intercept, slope and correlation coefficient were calculated using PRISM, version 6.0 (GraphPad Software Inc, La Jolla, CA, USA). The concentration of NBD-PC was calculated by a regression equation.

Time and enzyme concentration dependency of the recombinant hLPCAT3 catalyzed reaction

To investigate the enzyme concentration dependency, general reactions were carried out except for varied amount of purified recombinant hLPCAT3 from 0.03 to 2 µg·mL⁻¹. Velocity of the reaction (pmol·min⁻¹·U⁻¹) was plotted against the concentration of the enzyme. To investigate time dependency, general reactions were carried out except for varied reaction time from 5 to 180 min. Stage of initial velocity was determined by plotting the velocity of the formation of NBD-PC versus reaction time.

Effect of the pH and temperature on rhLPCAT3 enzyme activity

To investigate the effect of pH on the reaction, general reactions were carried out, except for a varied pH from 3.0 to 9.1. HCl or NaOH was used to adjust the pH of Tris-Cl buffer. To investigate the effect of temperature on the reaction, general reactions were carried out, except for a varied temperature from 0 to -60 °C. Velocity of the reaction ($\text{pmol}\cdot\text{min}^{-1}\cdot\text{U}^{-1}$) was plotted against pH or temperature, respectively.

Characterization of the sequential kinetic Bi–Bi mechanism of the rhLPCAT3 reaction

To determine the K_m of NBD-lyso-PC and Ara-CoA, general reactions were carried out except, for varied substrate concentrations. The kinetic mechanism and parameters of this Bi–Bi reaction were obtained by analyzing experimental Lineweaver-Burk plots containing 16 velocity points. The substrate Ara-CoA was held at several constant concentrations (0.75 – 9.00 μM) and the velocities were determined when the concentration of the substrate NBD-lyso-PC was varied from 20 to 100 μM .

Determination of the IC_{50} of the rhLPCAT3 inhibitor TSI-10

Recombinant human LPCAT3 enzyme activity was measured to screen effective inhibitors. The inhibitory activities of different concentrations of the compounds were determined in a standard 100 μL reaction mixture containing 1 $\text{mg}\cdot\text{mL}^{-1}$ BSA, 75 mM Tris-Cl (pH 6.0), 1 mM DDM, 11 $\mu\text{mol}\cdot\text{L}^{-1}$ NBD-lyso-PC, 11 $\mu\text{mol}\cdot\text{L}^{-1}$ Ara-CoA and purified rhLPCAT3 enzyme (one-unit). The reaction was carried out at 30 °C for 10 min. Concentration of product NBD-PC was analyzed by the HPLC and the IC_{50} of the inhibitors was calculated using PRISM, version 6.0.

Statistical analysis

The analyzed data were expressed as mean \pm SD. All statistical calculations were performed using Excel 2016 (Microsoft Corp., Redmond, WA, USA) or PRISM, version 6.0.

Results

Recombinant hLPCAT3 preparation

To achieve a premium enzyme source, we expressed the hLPCAT3 protein in Sf9 insect cells and purified the protein by taking advantage of the fused twin-strep tag in the C terminal of the rhLPCAT3. Analysis by

SDS/PAGE revealed that a band of about 60 kDa, the calculated MW of rhLPCAT3, consisted of the major component of the purified protein, although a trace amount of contaminant protein remained after the purification process (Fig. 1A). The activity assay by TLC showed that the recombinant protein has a high specific activity of lysophosphatidylcholine acyltransferase because only 1 μg of the purified protein produced NBD-PC identical to that obtained with 50 μg of microsomal proteins (Fig. 1B). Furthermore, the powerful phospholipase A1 activity that exists in microsomal proteins was removed by the purification process, as indicated by disappearance of the band of NBD-labelled free fatty acid (Fig. 1B). Although we have a TLC method for LPCAT3 activity measurement, it is not sufficiently sensitive. We used the rhLPCAT3 to establish a new sensitive method for LPCAT3 activity analysis.

The activity of rhLPCAT3 can be measured by reversed-phase HPLC with fluorescence detector

The enzymatic reaction product NBD-PC could easily be detected by the fluorescence detector. We identified an optimal mobile phase with methanol/water/trifluoroacetic acid (94:6:0.04, v/v) for separating product NBD-PC and substrate NBD-lyso-PC. The retention time is 10.782 min for the product NBD-PC and 2.884 min for the substrate NBD-lyso-PC (Fig. 1C). The product signal could be measured within a linear range up to 13 433 $\text{nmol}\cdot\text{L}^{-1}$ NBD-PC ($r^2 = 0.9988$) (Fig. 1D). To determine the activity of rhLPCAT3, we established a general catalytic reaction at pH 6.0, incubated at 30 °C for 10 min, using 100 $\mu\text{mol}\cdot\text{L}^{-1}$ NBD-lyso-PC and 100 $\mu\text{mol}\cdot\text{L}^{-1}$ arachidonoyl CoA in a 100 μL system. Different enzyme concentrations were used to investigate the enzyme concentration dependency on this condition. After mixing with equal volume of acetonitrile and centrifugation, the product NBD-PC in 20 μL of supernatant could be analyzed by reversed-phase HPLC. As shown in Fig. 2A, the formation of NBD-PC catalyzed by rhLPCAT3 is linear ($r^2 = 0.9959$) with the concentration of enzyme varying from 0.03 to 2 $\mu\text{g}\cdot\text{mL}^{-1}$, which means that the substrate concentration was sufficient to saturate the enzyme. To achieve uniform enzyme activity, we further defined one-unit of rhLPCAT3 activity (0.675 $\mu\text{g}\cdot\text{mL}^{-1}$) as the amount of enzyme required to generate 25 pmol NBD-PC $\cdot\text{min}^{-1}$ under general conditions.

To refine the catalytic reaction, the stage of initial velocity should be determined. Because one-unit of the purified protein could produce sufficient NBD-PC in

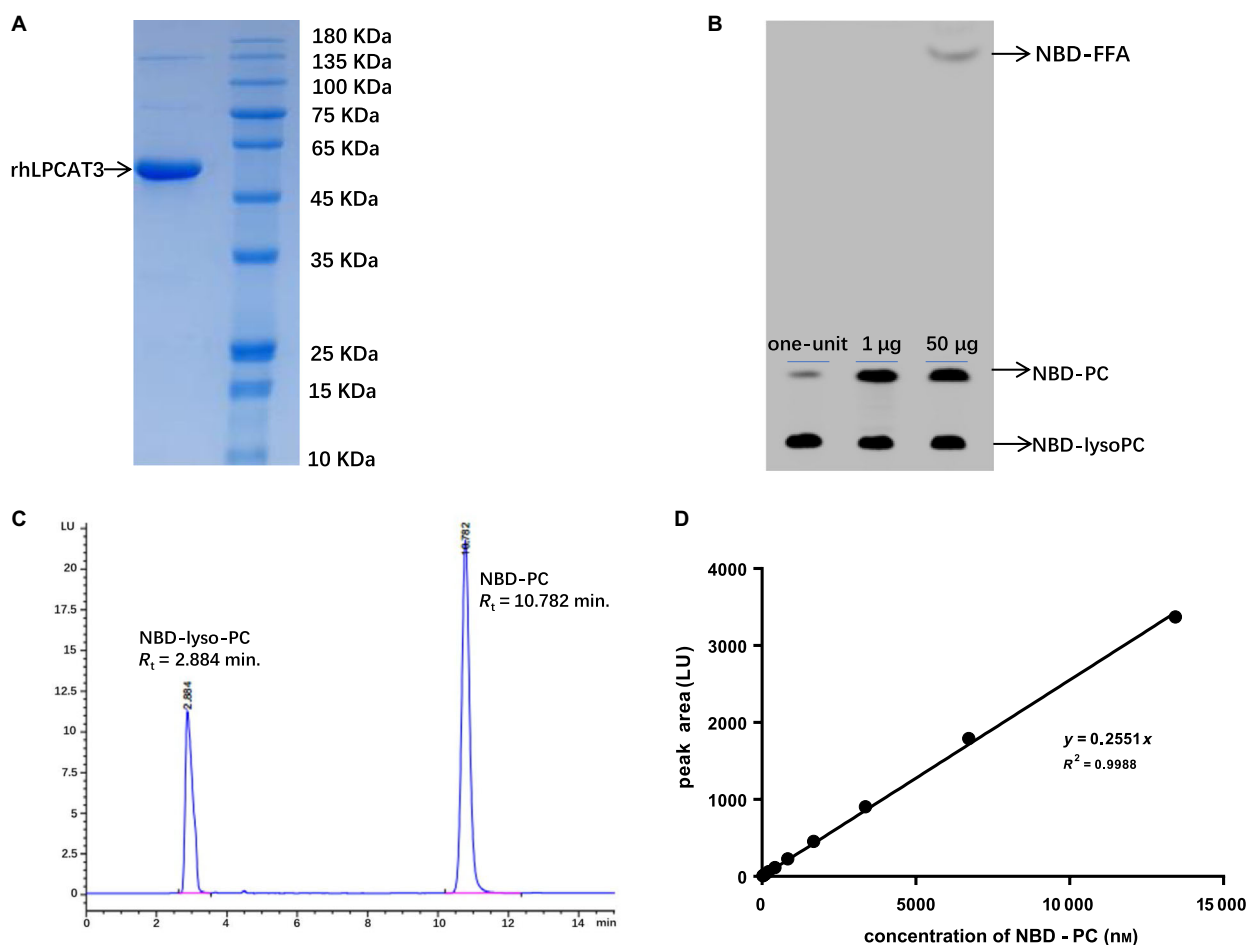


Fig. 1. The purified recombinant hLPCAT3 showed properties enabling it to be an ideal tool for an activity assay by reversed-phase HPLC. (A) rhLPCAT3 (60 kDa) identified by SDS/PAGE. (B) Activity comparison of rhLPCAT3 with liver microsomal proteins by TLC. From left to right: one-unit of hLPCAT3 (0.0675 μ g), 1 μ g of rhLPCAT3 and 50 μ g of liver microsomal protein in a 100 μ L reaction system. (C) The retention time (R_t) of NBD-lyso-PC ($R_t = 2.884$ min) and NBD-PC ($R_t = 10.782$ min) in the HPLC analysis. (D) The calibration curve of the peak area (y) versus the concentration of NBD-PC (x). The regression equation is $y = 0.2551x$, $r^2 = 0.9988$.

the presence of $100 \mu\text{mol}\cdot\text{L}^{-1}$ NBD-lyso-PC and $100 \mu\text{mol}\cdot\text{L}^{-1}$ Ara-CoA, we kept the reaction at 30°C and pH 6.0 for varying times from 5 to 180 min (Fig. 2B). The results obtained showed that the amount of NBD-PC increased at a fixed rate within 20 min, which indicated that all of the reactions in 20 min were in the stage of initial velocity (Fig. 2C). If only sufficient signal is produced for the HPLC measurement, a reaction time of 10 min was established for further experiments.

Kinetic parameters of the rhLPCAT3

Provided that other factors were fixed, alteration of the rhLPCAT3 activity versus the pH was performed as shown in Fig. 3A, which revealed an optimal pH of 6.0. Similarly, a change of rhLPCAT3 activity versus

temperature was determined, as shown in Fig. 3B, which revealed an optimal temperature of 30°C . Once the optimal pH and temperature were determined, we attempted to measure the K_m of NBD-lyso-PC and arachidonoyl CoA under this optimal condition. Because rhLPCAT3 used two molecules as its substrates, we calculated the K_m based on the Bi-Bi reaction mechanism. In the Lineweaver-Burk plots where the rates observed with different fixed concentration of NBD-lyso-PC are plotted versus a series of constant concentration of Ara-CoA, we found that the lines crossed at the same point on the left of $1/v$ axis, indicating a sequential mechanism rather than a ping-pong mechanism in this Bi-Bi enzymatic reaction. We calculated the kinetic constants by the Dalziel formula, as widely used in bisubstrate reactions. We obtained a series of intercept and slope by double reciprocal plots

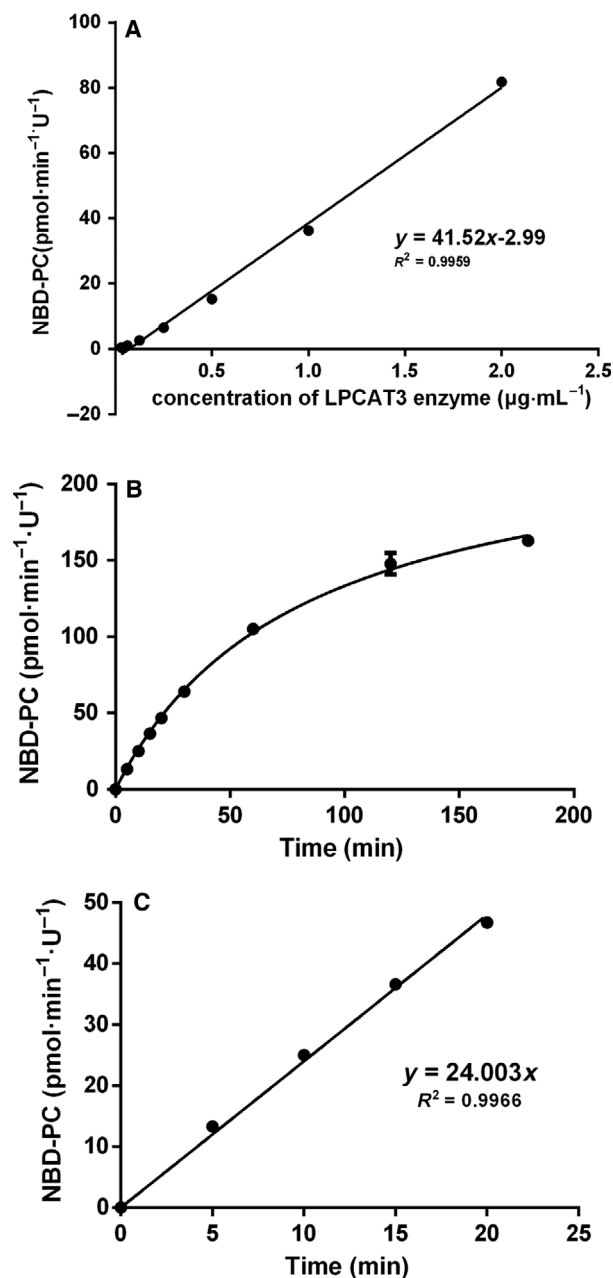


Fig. 2. Enzyme concentration and reaction time dependent velocity analysis. (A) Velocity analysis under different amounts of rhLPCAT3 (from 0.03 to 2 $\mu\text{g}\cdot\text{mL}^{-1}$). The curve is linear and the correlation coefficient is $r^2 = 0.9959$. (B) Velocity analysis of one-unit of rhLPCAT3 incubated at 30 °C and pH 6.0 with different reaction times (from 5 to 180 min). (C) The stage of initial velocity is up to 20 min.

of initial velocity versus [NBD-lyso-PC] at several fixed Ara-CoA concentrations (Fig. 4A). Next, the $\Phi_{\text{NBD-lyso-PC}}$ and $\Phi_{\text{NBD-lyso-PC}\cdot\text{Ara-CoA}}$ were obtained by the plot of slope versus $1/[\text{Ara-CoA}]$ (Fig. 4B), whereas $\Phi_{\text{Ara-CoA}}$ and Φ_0 were

obtained by the plot of intercept versus $1/[\text{Ara-CoA}]$ (Fig. 4C) ($\Phi_{\text{Ara-CoA}} = 0.2773$, $\Phi_0 = 0.02515$, $\Phi_{\text{NBD-lyso-PC}} = 6.711$, $\Phi_{\text{NBD-lyso-PC}\cdot\text{Ara-CoA}} = 2.302$). The classical kinetic constants can be calculated by transforming the Dalziel equation to the Albery equation: $V_{\text{max}} = 1/\Phi_0$ ($39.76 \text{ pmol}\cdot\text{min}^{-1}\cdot\text{U}^{-1}$); $K_m (\text{Ara-CoA}) = \Phi_{\text{Ara-CoA}}/\Phi_0$ ($11.03 \text{ }\mu\text{mol}\cdot\text{L}^{-1}$); $K_m (\text{NBD-lyso-PC}) = \Phi_{\text{NBD-lyso-PC}}/\Phi_0$ ($266.84 \text{ }\mu\text{mol}\cdot\text{L}^{-1}$) [18];

$$\text{Dalziel equation: } \frac{1}{V_0} = \Phi_0 + \frac{\Phi_B}{[B_0]} + \frac{\Phi_A}{[A_0]} + \frac{\Phi_{AB}}{[A_0] \cdot [B_0]}.$$

V_0 is the initial velocity; $[B_0]$ is the initial concentration of Ara-CoA; $[A_0]$ is the initial concentration of NBD-lyso-PC; Φ_0 , Φ_A , Φ_B and Φ_{AB} are kinetic constants.

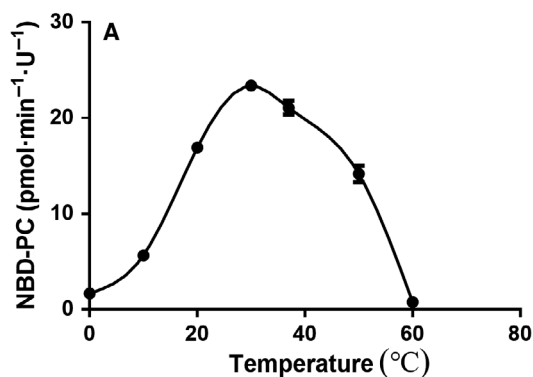
Determination of the efficiency of certain rhLPCAT3 inhibitors

Because the HPLC method was established and the kinetic parameters were determined, we attempted to unify the catalytic reactions to measure and compare the power of rhLPCAT3 regulators. In reactions where factors such as activity of recombinant hLPCAT3 protein, substrate concentrations, optimal pH and temperature and reaction time were kept the same, the apparent rhLPCAT3 activities were measured versus a series of concentrations of candidate compound. Furthermore, the LPCAT2 inhibitor TSIs were screened to confirm the inhibitory activity on rhLPCAT3 by this method. However, only TSI-10 showed inhibitory effects, with an example shown in Fig. 5A. The calculated IC_{50} value is shown in Fig. 5B.

Discussion

Subsequent to LPCAT3 being identified and cloned about 11 years ago, multiple evidence has been obtained revealing that, besides lyso-PC, this enzyme preferred polyunsaturated acyl CoA, especially arachidonoyl CoA, as its favorite substrate [2,19,20]. Although radioactivity labeled substrates or the LC/MS/MS analysis method could be used to determine the activity of LPCAT3, we have attempted to develop an easily performed alternative method, using fluorescent substrate NBD-lyso-PC to establish the catalytic reaction, followed by measurement of the product NBD-PC separated by TLC [6,7,9]. Lipids were usually separated by TLC in a normal phase pattern and a large amount of chloroform would be used as a reagent of development solvent. Chloroform can be harmful for health if researchers are not properly protected. Furthermore, performing TLC is labor

The effect of temperature on LPCAT3 enzyme activity



The effect of pH on LPCAT3 enzyme activity

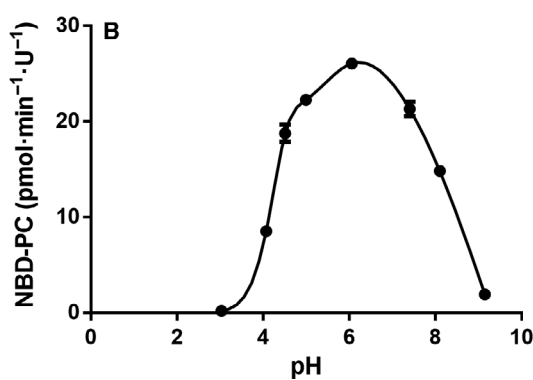


Fig. 3. Optimal conditions for enzymatic reactions. (A) The effect of temperature on the activity of the rhLPCAT3, with an optimal temperature of 30 °C. (B) The effect of pH on the activity of rhLPCAT3, with an optimal pH of 6.0. Values are mean \pm SD ($n = 3$).

consuming and the intensity of the target band on the plate could be measured in a semiquantitative way. By contrast, with the aid of HPLC machine, samples were loaded automatically and analyzed quantitatively, which provided a more accurate, sensitive and labor saving method. In practice, HPLC is more widely accepted in the reversed-phase pattern than in the normal phase pattern. Accordingly, when calculating the exact power of LPCAT3 regulators, we further developed a reversed-phase HPLC with a fluorescence detector to measure the product NBD-PC.

For screening compounds that regulate LPCAT3 activity, it is unsatisfactory to use tissue homogenate or microsome as the source of the enzyme because a large amount of substrate lyso-PC would be consumed rapidly by a powerful phospholipase A1 activity that exists in the endoplasmic reticulum to produce free fatty acid, with NBD labeled in this case (Fig. 1B). Jain *et al.* [19] had attempted to express the human

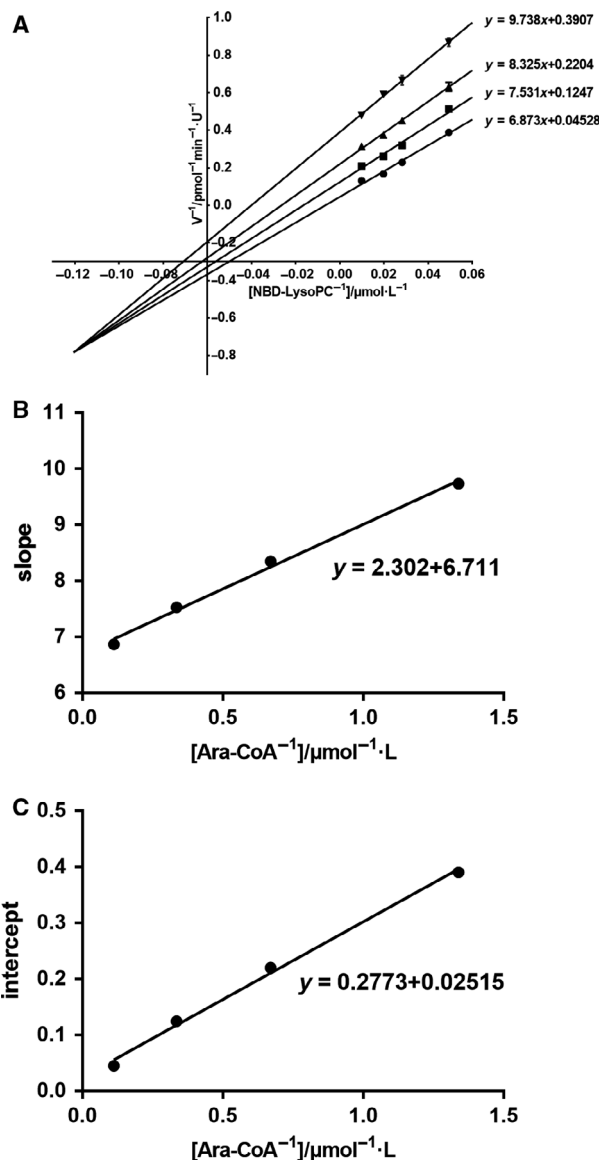


Fig. 4. Determination of enzyme kinetic parameters and identification of the reaction mechanism. (A) The double reciprocal of initial velocity versus [NBD-lyso-PC] at several constant Ara-CoA concentrations. (●) 9.00 $\mu\text{mol}\cdot\text{L}^{-1}$; (■) 3.00 $\mu\text{mol}\cdot\text{L}^{-1}$; (▲) 1.50 $\mu\text{mol}\cdot\text{L}^{-1}$; and (▼) 0.75 $\mu\text{mol}\cdot\text{L}^{-1}$. (B) Replots of slope as a function of $[\text{Ara-CoA}]^{-1}$. (C) Replots of intercept as a function of $[\text{Ara-CoA}]^{-1}$.

LPCAT3 in insect cells and harvest powerful activities from the cell homogenate [19]. We also expressed the human LPCAT3 in this Sf9 insect cells, with a Twin-Strep tag being fused with the C terminal of the target protein for further purification. Although a trace amount of contaminant proteins was not removed, the purified recombinant hLPCAT3 showed no phospholipase A1 activity, with a high specific activity to

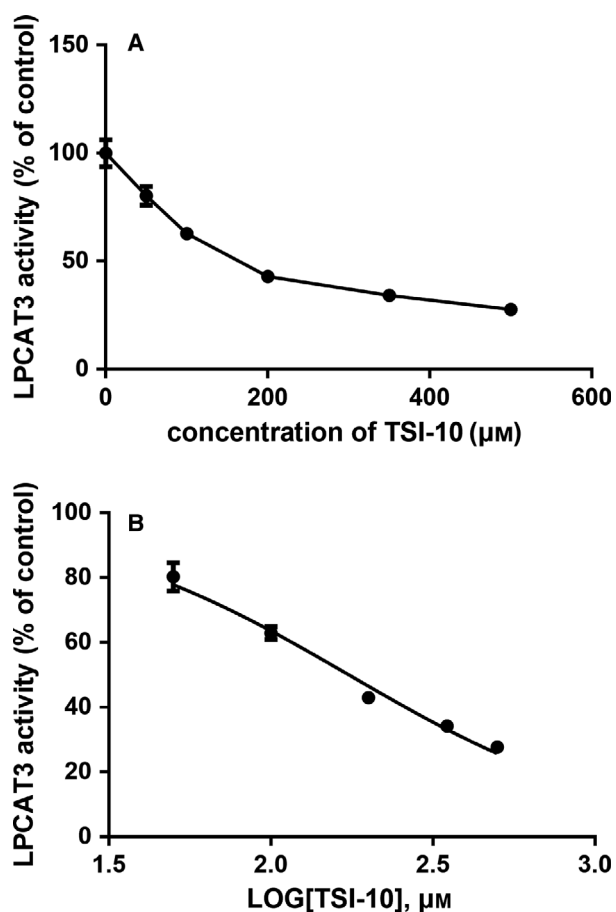


Fig. 5. Determination of inhibitor IC_{50} by HPLC. (A) Representation of the inhibition studies with the reaction mixture containing one-unit of rhLPCAT3, $11 \mu\text{mol}\cdot\text{L}^{-1}$ NBD-lyso-PC/Ara-CoA and a series of concentrations of TSI-10. (B) The IC_{50} was calculated using PRISM, version 6.0. Values are the mean \pm SD ($n = 3$). $IC_{50} = 174.00 \pm 1.04 \mu\text{mol}\cdot\text{L}^{-1}$.

produce NBD-PC. These properties suggest that the recombinant hLPCAT3 is an ideal tool for *in vitro* compound screening.

Because the combination of commercially available 12:0 NBD-lyso-PC with arachidonoyl CoA (when compared with palmitoyl CoA or oleoyl CoA) enables recombinant hLPCAT3 with the highest catalytic power (data not shown), we chose 12:0 NBD-lyso-PC and arachidonoyl CoA as the two substrates for a further rhLPCAT3 activity assay to produce a product of NBD-PC with a NBD-labeled dodecyl group (12:0) in the *sn*-1 position and arachidonoyl group (20:4) in the *sn*-2 position. The two substrates were dissolved in the methanol and could easily be distributed in the reaction buffer containing $1 \text{ mg}\cdot\text{mL}^{-1}$ BSA uniformly. This product NBD-12:0 20:4 PC (retention time = 10.782 min) was easily separated from the substrate

NBD-lyso-PC (retention time = 2.884 min) by reversed-phase HPLC with a mobile phase of methanol/ddH₂O/trifluoroacetyl acid (94:6:0.04, v/v). A higher methanol ratio in the mobile phase would cut down the retention time of NBD-PC and save machine time for HPLC analysis, although at the cost of shortening the life span of the C18 column. The molar mass of NBD-PC was determined by the fluorescence signal presenting a peak area within the linear range as high as 3300 LU (Fig. 1D).

When substrate and enzyme concentrations were fixed, the product NBD-PC is linearly proportional to the reaction time up to 20 min (Fig. 2B,C). This suggested that all of the reactions within 20 min proceeded at the initial velocity. A 10 min reaction time was unified in further experiments. When substrates are fixed as $100 \mu\text{mol}\cdot\text{L}^{-1}$ NBD-lyso-PC and $100 \mu\text{mol}\cdot\text{L}^{-1}$ arachidonoyl CoA, respectively, the product NBD-PC is linearly proportional to an enzyme concentration as high as $2 \mu\text{g}\cdot\text{mL}^{-1}$ protein (Fig. 2A). This result suggested that recombinant hLPCAT3 enzymes up to $2 \mu\text{g}$ protein $\cdot\text{mL}^{-1}$ were saturated by the substrates at the indicated concentration. Based on these data, a primary protocol of the recombinant hLPCAT3 at as little as $0.657 \mu\text{g}\cdot\text{mL}^{-1}$ protein (one-unit), NBD-lyso-PC $100 \mu\text{mol}\cdot\text{L}^{-1}$ and arachidonoyl CoA $100 \mu\text{mol}\cdot\text{L}^{-1}$ was settled to establish the catalytic reaction because the fluorescence signal output was sufficiently sensitive for quantitative analysis. Under this condition, we identified an optimal pH of 6.0 and an optimal temperature of 30 °C. Jain *et al.* [19] had also reported a five-fold higher activity at 28 °C than at 37 °C, although they performed the reaction at pH 7.4. We further determined the K_m of NBD-lyso-PC and arachidonoyl CoA by the model of Bi-Bi reaction under optimal conditions. Because the apparent K_m of one substrate is affected by the concentration of another in the Bi-Bi reaction, we obtained theoretical K_m values of $266.84 \mu\text{mol}\cdot\text{L}^{-1}$ for NBD-lyso-PC and $11.03 \mu\text{mol}\cdot\text{L}^{-1}$ for arachidonoyl CoA by the Dalziel equation. The K_m value of arachidonoyl CoA is comparable with that reported by Zhao *et al.* [2,19], with an apparent K_m of about $72 \mu\text{mol}\cdot\text{L}^{-1}$ at 37 °C and pH 7.5, and also that reported by Jain *et al.* [2,19], with an apparent K_m of $55.8 \mu\text{mol}\cdot\text{L}^{-1}$ at 28 °C and pH 7.4, and an apparent K_m of $245 \mu\text{mol}\cdot\text{L}^{-1}$ at 37 °C and pH 7.4. Regarding the K_m of the NBD-lyso-PC that we determined, a comparable K_m for 1-palmitoyl lyso-PC of $72.19 \mu\text{mol}\cdot\text{L}^{-1}$ was also reported by Zhao *et al.* [2] under a reaction condition of 37 °C and pH 7.5. However, the theoretical K_m values calculated by Bi-Bi kinetic equations were more accurate than that

calculated by the Michaelis–Menten equation because the apparent K_m of one substrate calculated by the Michaelis–Menten equation may be influenced by the concentration of another, whereas Bi–Bi kinetic equations could overcome this disadvantage. Furthermore, from the Lineweaver–Burk plots where the rates observed with different fixed concentrations of one substrate Ara-CoA are plotted versus a series of concentrations of another substrate NBD-lyso-PC, a sequential kinetic mechanism could be proposed because plots of $1/v$ versus $1/[NBD\text{-lyso-PC}]$ at various constant values of $[Ara\text{-CoA}]$ (Fig. 4A) and $1/v$ versus $1/[Ara\text{-CoA}]$ at various constant values of $[NBD\text{-lyso-PC}]$ both converge to the left of the $1/v$ axis (data not shown), excluding the ping-pong mechanism, which is characterized by parallels. The sequential kinetic mechanism suggests that all substrates must bind prior to the release of any products. The ping-pong kinetic mechanism indicates that the product of the first reaction step is released from the enzyme before the other substrate binds. However, we can only infer a sequential Bi–Bi kinetic mechanism from Fig. 4A. The random Bi–Bi sequential mechanism and the ordered ternary complex sequential mechanism and the Theorell–Chance-type mechanism cannot be distinguished by the initial-rate method individually. This limitation arises from the insensitivity of initial-rate kinetics to the occurrence of internal isomerization reactions. Therefore, the distinct order of two substrates binds to the enzyme and product release remains to be explored.

In our general catalytic reactions, the concentration of both two substrates was settled at $100\ \mu\text{mol}\cdot\text{L}^{-1}$. As far as arachidonoyl CoA was concerned, this concentration was about 10-fold of its K_m , which was sufficiently high for kinetic analysis of the rhLPCAT3 enzyme. However, $100\ \mu\text{mol}\cdot\text{L}^{-1}$ of NBD-lyso-PC more or less reaches its K_m , which imposes an inevitable fault on the kinetic analysis. However, more NBD-lyso-PC was difficult to add because of the poor solubility of this substrate.

Because any change of the factors would have an effect on the signal output, it is essential to refine factors such as reaction time, concentration of substrates, and enzyme, pH and temperature to meet the requirements of the rhLPCAT3 activity assay or *in vitro* compound screening. We considered one-unit of rhLPCAT3 activity in our laboratories as that producing $25\ \text{pmol NBD-PC}\cdot\text{min}^{-1}$ at $30\ ^\circ\text{C}$ and pH 6.0 under a concentration of NBD-lyso-PC of $100\ \mu\text{mol}\cdot\text{L}^{-1}$ and arachidonoyl CoA of $100\ \mu\text{mol}\cdot\text{L}^{-1}$, respectively. In this standard, the specific activity of different batches of enzyme source should be determined before one-unit

of LPCAT3 activity was maintained for all of the experiments, which is essential for achieving comparable data.

Once enzyme activity was kept constant for all reactions, the concentration of the substrates became the prime factor that affected the values of IC_{50} as far as inhibitors were concerned. We modified the concentration of the substrates in our inhibitor screening experiments, keeping both NBD-lyso-PC and Ara-CoA as $11\ \mu\text{mol}\cdot\text{L}^{-1}$, which is equal to the K_m of Ara-CoA. This modification not only met the requirement for sensitive analysis, but also prevented unnecessary reagent consumption.

Acknowledgements

This work was supported by general projects of National Natural Science Foundation of China 31670849 (to YC), 81773576 (to YL) and 31770864 (to JD).

Conflict of interest

The authors declare no conflict of interest

Author contributions

YL, YC and TD conceived the project. XD, JH, BL, JD contributed to the design and coordination of experiments. XD, JH, QZ, QL, XX, SH, XG were directly involved in experimental data acquisition. JH and TD write the manuscript. All authors reviewed the results and approved the final version of the manuscript submitted for publication.

References

- 1 Shindou H, Hishikawa D, Harayama T, Eto M and Shimizu T (2013) Generation of membrane diversity by lysophospholipid acyltransferases. *J Biochem* **154**, 21–28.
- 2 Zhao Y, Chen YQ, Bonacci TM, Bredt DS, Li S, Bensch WR, Moller DE, Kowala M, Konrad RJ and Cao G (2008) Identification and characterization of a major liver lysophosphatidylcholine acyltransferase. *J Biol Chem* **283**, 8258–8265.
- 3 Ishibashi M, Varin A, Filomenko R, Lopez T, Athias A, Gambert P, Blache D, Thomas C, Gautier T, Lagrost L *et al.* (2013) Liver x receptor regulates arachidonic acid distribution and eicosanoid release in human macrophages: a key role for lysophosphatidylcholine acyltransferase 3. *Arterioscler Thromb Vasc Biol* **33**, 1171–1179.

- 4 Demeure O, Lecerf F, Duby C, Desert C, Ducheix S, Guillou H and Lagarrigue S (2013) Regulation of LPCAT3 by LXR. *Gene* **470**, 7–11.
- 5 Singh AB and Liu J (2017) Identification of hepatic lysophosphatidylcholine acyltransferase 3 as a novel target gene regulated by peroxisome proliferator-activated receptor δ . *J Biol Chem* **292**, 884–897.
- 6 Li Z, Ding T, Pan X, Li Y, Li R, Sanders PE, Kuo MS, Hussain MM, Cao G and Jiang XC (2012) Lysophosphatidylcholine acyltransferase 3 knockdown-mediated liver lysophosphatidylcholine accumulation promotes very low density lipoprotein production by enhancing microsomal triglyceride transfer protein expression. *J Biol Chem* **287**, 20122–20131.
- 7 Li Z, Jiang H, Ding T, Lou C, Bui HH, Kuo MS and Jiang XC (2015) Deficiency in lysophosphatidylcholine acyltransferase 3 reduces plasma levels of lipids by reducing lipid absorption in mice. *Gastroenterology* **149**, 1519–1529.
- 8 Jiang H, Li Z, Huan C and Jiang XC (2019) Macrophage lysophosphatidylcholine acyltransferase 3 deficiency-mediated inflammation is not sufficient to induce atherosclerosis in a mouse model. *Front Cardiovasc Med* **5**, 192.
- 9 Feng C, Lou B, Dong J, Li Z, Chen Y, Li Y, Zhang X, Jiang XC and Ding T (2018) Lysophosphatidylcholine acyltransferase 3 deficiency impairs 3T3L1 cell adipogenesis through activating Wnt/ β -catenin pathway. *Biochim Biophys Acta Mol Cell Biol Lipids* **1863**, 834–843.
- 10 Wang B, Rong X, Palladino END, Wang J, Fogelman AM, Martín MG, Alrefai WA, Ford DA and Tontonoz P (2018) Phospholipid remodeling and cholesterol availability regulate intestinal stemness and tumorigenesis. *Cell Stem Cell* **22**, 206–220.
- 11 Kakisaka K, Suzuki Y, Fujiwara Y, Suzuki A, Kanazawa J and Takikawa Y (2019) Caspase-independent hepatocyte death: a result of the decrease of lysophosphatidylcholine acyltransferase 3 in non-alcoholic steatohepatitis. *J Gastroenterol Hepatol* **34**, 1256–1262.
- 12 Taniguchi K, Hikiji H, Okinaga T, Hashidate-Yoshida T, Shindou H, Ariyoshi W, Shimizu T, Tominaga K and Nishihara T (2015) Essential role of lysophosphatidylcholine acyltransferase 3 in the induction of macrophage polarization in PMA-treated U937 cells. *J Cell Biochem* **116**, 2840–2848.
- 13 Kabir I, Li Z, Bui HH, Kuo MS, Gao G and Jiang XC (2016) Small intestine but not liver lysophosphatidylcholine acyltransferase 3 (Lpcat3) deficiency has a dominant effect on plasma lipid metabolism. *J Biol Chem* **291**, 7651–7660.
- 14 Tanaka H, Zaima N, Sasaki T, Yamamoto N, Inuzuka K, Yata T, Iwaki T, Umemura K, Sano H, Suzuki Y *et al.* (2017) Lysophosphatidylcholine acyltransferase-3 expression is associated with atherosclerosis progression. *J Vasc Res* **54**, 200–208.
- 15 Thomas C, Jalil A, Magnani C, Ishibashi M, Queré R, Bourgeois T, Bergas V, Ménégaut L, Patoli D, Le Guern N *et al.* (2018) LPCAT3 deficiency in hematopoietic cells alters cholesterol and phospholipid homeostasis and promotes atherosclerosis. *Atherosclerosis* **275**, 409–418.
- 16 Wang B and Tontonoz P (2019) Phospholipid remodeling in physiology and disease. *Annu Rev Physiol* **81**, 165–188.
- 17 Tarui M, Shindou H, Kumagai K, Morimoto R, Harayama T, Hashidate T, Kojima H, Okabe T, Nagano T, Nagase T *et al.* (2014) Selective inhibitors of a PAF biosynthetic enzyme lysophosphatidylcholine acyltransferase 2. *J Lipid Res* **55**, 1386–1396.
- 18 Purich DL (2010) *Enzyme Kinetics: Catalysis & Control [M]*. Elsevier Academic Press, Oxford. chapter5-6.
- 19 Jain S, Zhang X, Khandelwal PJ, Saunders AJ, Cummings BS and Oelkers P (2009) Characterization of human lysophospholipid acyltransferase 3. *J Lipid Res* **50**, 1563–1570.
- 20 Martin SA, Gijón MA, Voelker DR and Murphy RC (2014) Measurement of lysophospholipid acyltransferase activities using substrate competition. *J Lipid Res* **55**, 782–791.